Critical dimension for the dislocation structure in deformed copper micropillars

X. X. Zhao[a], J. Wu[a], Y. L. Chiu[a], I. P. Jones[a]*, R. Gu[b], A. H. W. Ngan[c]

[a]School of Metallurgy and Materials, University of Birmingham, Edgbaston, Birmingham, B15 2TT, UK

[b]Materials Characterization and Preparation Center, Southern University of Science and Technology, No. 1088, Xueyuan Road, Shenzhen, Guangdong, PR China

[c]Department of Mechanical Engineering, The University of Hong Kong, Pokfulam Road, Hong Kong, PR China

* Corresponding author. Email: j.wu.6@bham.ac.uk

ABSTRACT

Although the effect of specimen size on strength has been well documented for metal micro-samples significantly larger than ~1 μm, less is known about the deformation induced dislocation structure, especially just above the size at which dislocation starvation happens. Here, uniaxial compression tests were performed on cylindrical [011] oriented copper micropillars with diameters of 1 μm, 3 μm and 5 μm. Dislocation cells formed in a fractal geometry in the 3 μm and 5 μm pillars, while dislocations were not retained in the 1 μm pillars. This critical dimension for the change in dislocation structure is responsible for the different stress-strain behaviours observed. The effects of strain and strain rate on cell formation were also investigated.

Keywords: copper; micropillar; dislocation cell; fractal; focussed ion beam (FIB)

The deformation behaviour of metals has been investigated extensively in the micron and sub-micron regimes over the past decade. For FCC metals, samples smaller than ~ 1 μm in general exhibit the dislocation starvation phenomenon [1,2,3], where dislocations escape easily through free surfaces, leaving the sample in a continuously dislocation-starved state [4]. In this regime, the strength data usually exhibit significant scatter [5-7], thus preventing a clear size effect from being recognised. However, theoretical considerations do show the possibility of a "smaller is stronger" size effect, due to the continuous need to nucleate new dislocations to sustain deformation and yet, potential nucleation sites are more scarce in a smaller sample [8]. In FCC metal samples larger than ~1 μm, dislocation storage usually takes place, and in this regime, a clear "smaller is stronger" trend is consistently observed, in which the flow stress exhibits a power-law dependence on the sample size with the power exponent ranging from -0.4 to -1.0, depending on the material [9, 10-12] as well as on the initial dislocation content (i.e. pre-strain) in the sample [13-15]. In this dislocation storage regime, the size effect is generally thought to be due to a source truncation mechanism – dislocation sources are truncated by the free surfaces forming single ended Frank-Read sources. Such sources are on average shorter in a smaller sample and thus a higher applied stress is needed to activate them [2,16]. In addition, intermittent deformation of micro-samples is manifested by pronounced strain bursts and a corresponding stochastic scatter in the stress-strain curves [5-7,17-19].

Despite the general understanding of FCC micro-plasticity as outlined above, in the regime with dislocation storage (i.e. size > 1 μm), much less is known about the dislocation structure in the sample. Take copper as an example: in the bulk form it is a material in which dislocation subcells can form easily during deformation; it has also been reported that the subcell structure can exhibit a remarkable fractal pattern [20]. In fact, it has been postulated recently that Taylor hardening within a small sample containing a fractal dislocation subcell structure would lead to an exact power-law relation between the flow stress and the sample size, with the power exponent being inversely related to the fractal dimension of the subcell structure [13].

To date, only a limited number of studies have examined dislocation microstructures in micro-samples with sizes above 1 μm [21,22], and there is no clear indication of whether conventional subcells can form in such micro-samples and, if they do, whether their size will be affected by the sample size. Since it is known that samples smaller than ~1 μm do not store dislocations and hence do not exhibit subcells, in this work we focus on the dislocation structure in samples just larger than this critical size, namely, in Cu micropillars of 1, 3 and 5 μm diameter. The pillar orientation was chosen to be near a <110> direction – the single

crystal micropillars were FIB milled from within a large grain chosen from an EBSD map and this grain was indexed more exactly as [156].

A polycrystalline Cu (99.99% purity) sheet of approximately 2.5 mm $\times$ 1.5 mm $\times$ 0.5 mm was annealed at 850 °C for 24 hours in vacuum to encourage grain growth. It was then gradually ground and polished down to a 1 μm finish, followed by electropolishing using a 2:1 v/v mixture solution of H_3PO_4/H_2O at a constant voltage of 2 V for 5-10 minutes to produce a relatively smooth surface. Electron backscattered diffraction (EBSD) was performed on the polished sample to select grains from which the cylindrical micropillars could be prepared.

Compression was carried out using Hysitron PI85 picoindenter installed in a Tescan Mira II SEM with a flat punch under displacement control. To investigate the effect of sample size on the cell formation, 1, 3 and 5 μm diameter pillars were compressed at a strain rate of 10^{-3} s^{-1} to 8% strain. In addition, 3 μm diameter pillars were compressed to 4% and 16% strains at a strain rate of 10^{-3} s^{-1}, and, separately, 3 μm pillars were compressed to 8% strain using strain rates of 10^{-2} s^{-1}, 10^{-3} s^{-1} and 10^{-4} s^{-1} to study the effect of strain and strain rate on cell formation.TEM specimens were FIBbed from the deformed micro-pillars and examined via STEM using an FEI Talos F200.

The pillar diameters measured at half sample height position were approximately 1, 3 and 5 μm. In addition, every pillar was slightly tapered (smaller at the top). Typical stress-strain curves obtained from [156] single crystal cylindrical pillars are shown in Figure 1. All the tests were repeated many times and the mechanical response shows considerable scatter, especially as the sample size shrinks. Overall, evident from the curves is a "smaller is stronger" trend, i.e., the flow stress increases with decreasing sample size, which has commonly been observed in fibbed small-scale samples [11,23-25]. The power exponent deduced from log-log plots at 0.05 strain is -0.45±0.11 which is in line with recent experiments on Cu microcrystals [12]. With a 10^{-3} s^{-1} strain rate, it is noticed that lots of strain bursts occur during the compression of 1 μm and 3 μm diameter pillars, but smoother curves are obtained with 5 μm diameter pillars. Also the 5 μm diameter pillar shows higher work hardening compared to the 3 μm diameter pillars. With the different strain rates, the 3 μm diameter pillars show similar mechanical responses.
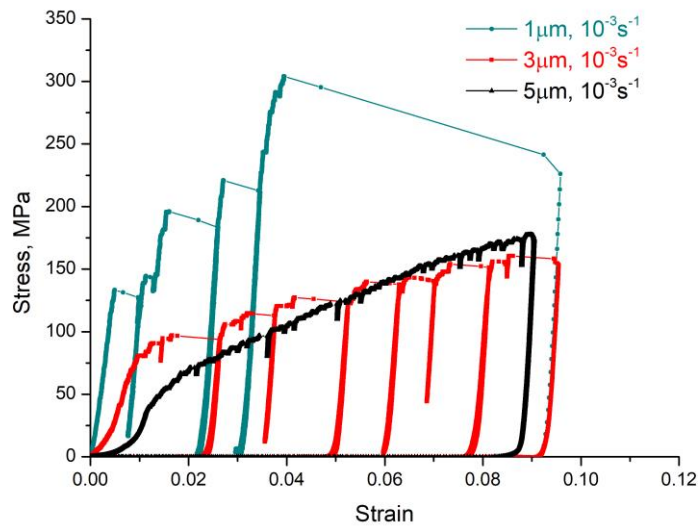
Figure 1 Stress-strain curves of the Cu pillars with different diameters and strain rates.

SEM images showed that in most cases slip bands form on two different sets of planes, which correspond to the two highest Schmid factors, while in a few cases deformation occurs preferentially on one set of planes only. Fig. 2 shows a typical pillar with a diameter of 3 μm where slip on (111) and $(\bar{1}11)$ is evident. The number of activated slip systems does not depend on the strain level, as multiple slip develops in samples with the smallest strains as well. No obvious difference in the appearance of the slip bands was found between the samples with different diameters. There was no obvious connection between single/double slip and specimen size as the simulations of Ng and Ngan [11] and the observations of Kiener and Minor [7] would suggest, but this may be due to inadequate statistics.
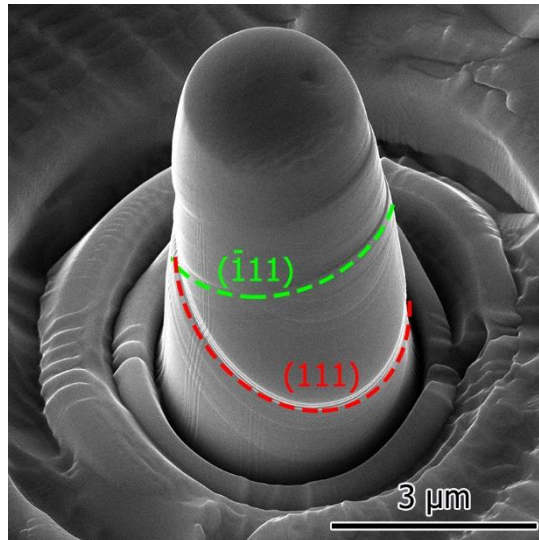
Figure 2 SEM image of a 3 μm diameter [156] cylindrical pillar deformed to ~7.8% strain with strain rate of 10^{-3} s^{-1}. Images were taken at a tilt of 30˚.

To assess the evolution of the dislocation structure during deformation, a knowledge of the initial dislocation arrangement in the undeformed sample is important. To this end, a thin foil was extracted from an undeformed 2.6 μm diameter micropillar. The dislocations were non-uniformly distributed inside the pillar: some regions contain a relatively high density of dislocations while others are completely free of dislocations. Therefore, various initial dislocation distributions may exist in different micro-pillars and this may contribute to the scatter in their mechanical behaviour. The initial average dislocation density ρ_0 was measured to be $\sim 1.3 \times 10^{13}$ m^{-2}.

Figure 3(a) shows the TEM specimen extracted from a 1 μm pillar after 9.1 % deformation. Leaving aside the tangle of dislocations top right (probably caused by local stress concentration at the contact surface between the pillar and indenter), a large portion of the pillar is virtually dislocation free. The overall density of dislocations was $\sim 2.3 \times 10^{12}$ m^{-2}, rather less than the grown-in density. This agrees with the dislocation starvation narrative proposed by Greer et al. [4]. The dislocations which produced the large slip steps in Figure 2(a) have come and gone.

Figure 3(b) shows the dislocation structure in a 3 μm pillar after deformation to 8.1% strain. A dislocation cell structure is starting to form, with a cell size of approximately 1 μm. The dislocation structure in Figure 3(b) appears not to relate to the coarse slip steps of Figure 2. Perhaps the formation of a macroscopic slip step implies easy transfer of the dislocations involved across the pillar and thus that, again, as in the 1 μm pillar, the dislocations

responsible for the slip step have come and gone. This is consistent with Kirchlechner et al.'s reported observations on copper [26]. The overall dislocation density in the 3 μm pillar was $\sim 3.6 \times 10^{13}$ m^{-2}.

Figure 3(c) shows the dislocation structure in a 5 μm pillar after 8.0% strain. The cells are well developed and the size of the cells is at about half a micron across, which are smaller than those in the 3 μm 8.1% strain pillar. The dislocation density was estimated to be $\sim 1.0 \times 10^{14}$ m^{-2}.

Figures 3 (d) and (e) show the dislocation structure in a 3 μm pillar after different strains. With 4% strain (Figure 3d), the dislocations are distributed inhomogeneously but no obvious cells were formed, and the dislocation density was estimated to be $\sim 1.6 \times 10^{13}$ m^{-2}. With 8% strain (Figure 3b), the residual dislocations started to accumulate and form some cell boundaries. This becomes more evident with pillars of 16% strain (Figure 3e); cells form and remain in the centre of the pillar with cell boundaries reaching out. Dislocations tangles form cell boundaries which appear rather dark compared with the matrix, and the dislocation density was $\sim 2.5 \times 10^{13}$ m^{-2}. Interestingly, in this specimen the areas outside the cell boundaries remain dislocation free, but we are not suggesting that this is a necessary progression from fig. 3(b) to fig. 3(e). The cell size decreases with strain.

Figures 3(f) and (g) illustrate the effect of strain rate on cell formation. In fact, there is not much. The dislocation densities were estimated to be $\sim 2.2 \times 10^{13}$ m^{-2} and $\sim 3.1 \times 10^{13}$ m^{-2} for figs 3(f) and 3(g) respectively, which are similar to the value for fig. 3(b). Again, as with fig. 3(e), there is a tendency in figs 3(f) and 3(g) for cell formation or retention to be in the centre of the pillar.
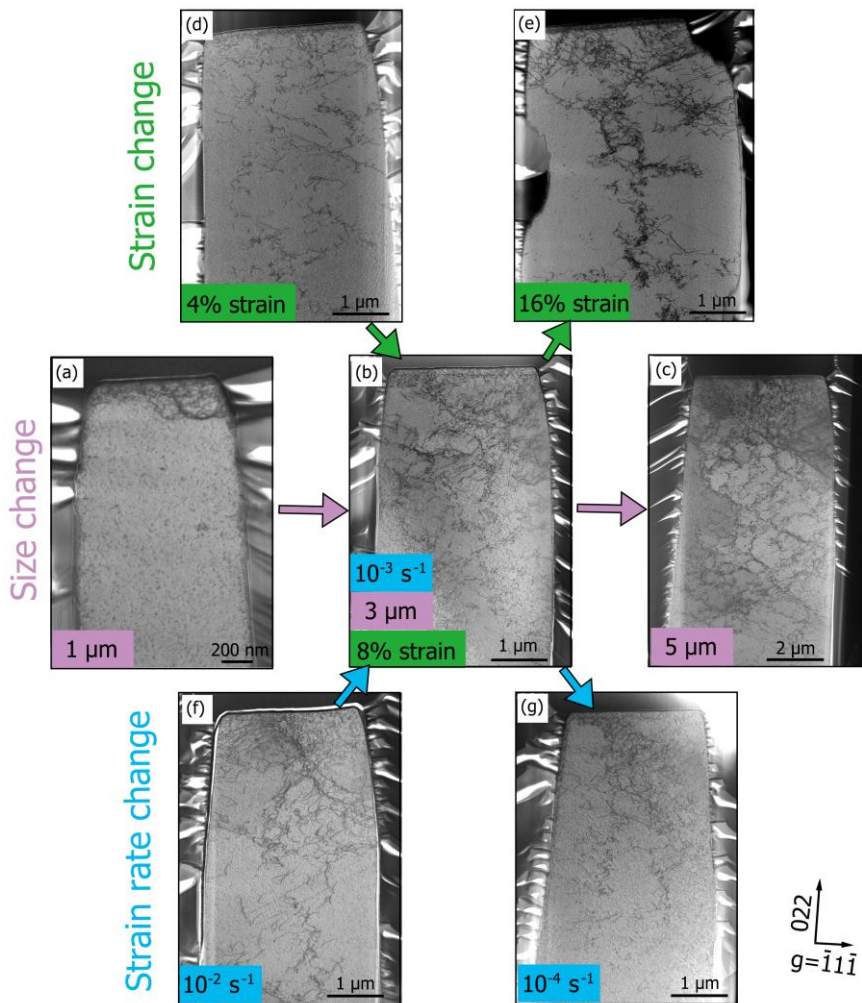
Figure 3 Bright field STEM images showing morphologies of compressed micropillars with different diameters, strain rates and total strains with the same beam condition of $g=\bar{1}1\bar{1}$, BD~$[21\bar{1}]$: (a) 1 μm cylindrical pillar after 9.1% strain with strain rate of 10^{-3} s^{-1}; (b) 3 μm, 8.7% strain, 10^{-3} s^{-1} strain rate; (c) 5 μm, 8.0% strain, 10^{-3} s^{-1} strain rate ; (d) 3 μm, 4.3% strain, 10^{-3} s^{-1} (e) 3 μm, 16.7% strain, 10^{-3} s^{-1} strain rate; (f) 3 μm, 7.2% strain, 10^{-2} s^{-1} strain rate; (g) 3 μm, 7.3% strain, 10^{-4} s^{-1} strain rate.

There is a change in the strength response between the 1 μm and 3 μm samples. Dislocation source activation controls the deformation below 1 μm and dislocation interactions are significant above it. The critical size for this dislocation cell structure is similar to the cell size, as might perhaps have been expected. The average cell size measured from this sample is about 1 μm, which is consistent with dislocations being unlikely to be trapped in samples with a dimension of, or smaller than, 1 μm.

Our observations are more consistent with the cell formation mechanism of Hansen and Kuhlmann-Wilsdorf [27] than with that of Holt [28] in that the cells appear to form gradually, not via one event.

7

Our observations of the 1 μm pillars show that not only are few dislocations left in the pillars, but also that what dislocations there were at the beginning are almost totally removed. In the 3 μm and 5 μm specimens, although there is a considerable density of dislocations remaining, there is no obvious connection between their structure and the external slip steps created by the strain bursts. Thus our observations are that the number of dislocations from the strain burst remaining in the specimen is fairly small. The larger pillars exhibit a lower strength but much higher dislocation density; this trend between strength and dislocation density is opposite to the Taylor mechanism where more mobile dislocations should produce strengthening. It is possible that strength in the size range studied is controlled by the single-ended Frank-Read sources, the operating stress of which exhibits an inverse scaling with the source length [2, 16]. However, the vast difference in dislocation storage between the 1 μm pillars and larger ones after deformation suggests that dislocation interactions and work hardening should be very different in the two cases. A previous study has shown that the strength of 5.6 μm aluminium pillars was proportional to the square-root of the dislocation density which was varied by pre-straining and pillar-coating treatments, but the dislocation density of 1.2 μm pillars could not be changed by similar treatments and their strength was not correlated with the dislocation density [ref. R. Gu and A.H.W. Ngan, Acta Mater. 60 (2012) 6102]. This shows that Taylor hardening can be significant in larger pillars with sufficient dislocation storage, while it plays little role in pillars around 1 μm in size.

Figures 4 (a-c) show the results of a box-counting analysis of the STEM images. The STEM images were converted into binary format, and then the digitized bitmap was covered by successive sets of grids with decreasing side length Δx, and the number of boxes $N(\Delta x)$ containing at least one dislocation were calculated. If the dislocation arrangement is in a fractal geometry, $N(\Delta x)$ should decrease with increasing side length Δx according to a power-law relation. Δx ranges from ~20nm to ~400nm; this range would represent a reasonable internal length scale of the dislocation microstrutures in the deformed micro-pillars. Fig. 4(a) illustrates the *size effect* on the dislocation distribution for pillars deformed to similar strains at a similar strain rate as shown in fig. 3(a)-(c). For the 1μm case, the double-logarithmic plot of $N(\Delta x)$ with Δx is not quite linear, indeed rather jerky, while for the 3μm and 5μm cases, the double-logarithmic plots become very smooth and linear. This result suggests that when the pillar size is large enough - close to or greater than 3μm in diameter - the dislocation segments arrange in a fractal manner. The slopes of curves in the plot, i.e. the values of Λ_B, were measured to be 1.371 ± 0.028, 1.516 ± 0.006, and 1.695 ± 0.004, for 1μm, 3μm and 5μm pillars respectively, as Δx ranges from ~20nm to ~400nm: this range may represent a

reasonable value of spacing between dislocation segments. The Λ_B of the 3µm and 5µm pillar sizes are therefore similar but that of the 1 µm pillar size is significantly lower. Since Λ_B serves as a quantitative marker of the cellular structure of the dislocations [20], the results here confirm that the dislocation configuration in the 1 µm pillar size is significantly different from that in the larger pillars.

Figure 4(b) shows the box-counting analysis on a 3µm pillar at different *strains* corresponding to the STEM images in figure 3(d), 3 (b) and 3(e). The three curves are approximately linear, while for the 4% strain case, the slope of the curve is obviously lower than for the other two pillars. The measured Λ_B are 1.345 ± 0.002, 1.516 ± 0.006 and 1.596 ± 0.002 for 4%, 8% and 16% strain respectively. This result Indicates that dislocation fractal cellular structures evolved with increasing strain during deformation.

Figure 4(c) illustrates the effect of *strain rate* on the results of the box-counting analysis, corresponding to the STEM images in figures 3(f), 3(b) and 3(g). The double-logarithmic plots of N(Δx) with Δx for the three pillars are quite close, although Λ_B for the $10^{-2}s^{-1}$ strain rate case was measured to be 1.654 ± 0.003. This is obviously greater than the values of the $10^{-3}s^{-1}$ and $10^{-4}s^{-1}$ cases, which have similar Λ_B of 1.516 ± 0.006 and 1.492 ± 0.006 respectively. This shows that strain rate is not the principal factor controlling the dislocation arrangement when the pillar is deformed in a quasi-steady manner.
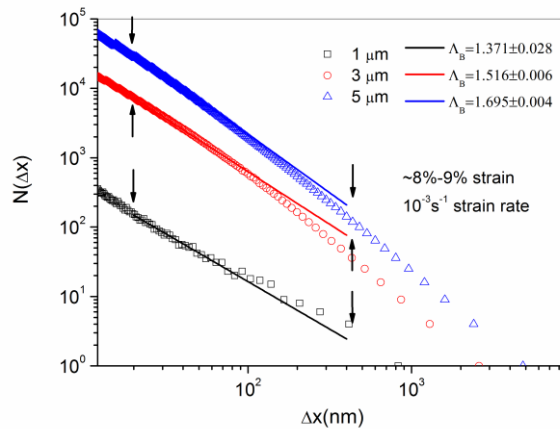
(a)
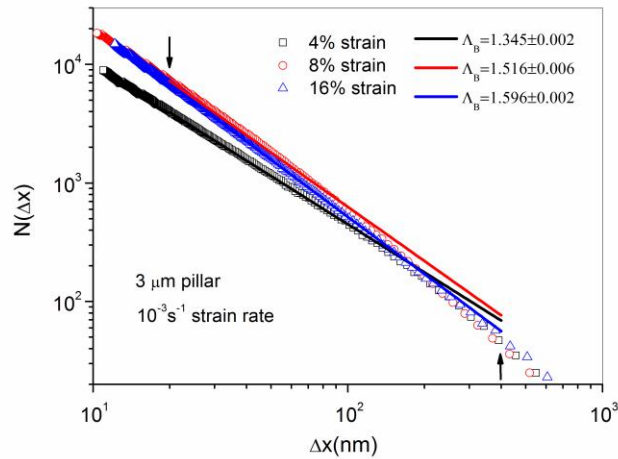
(b)
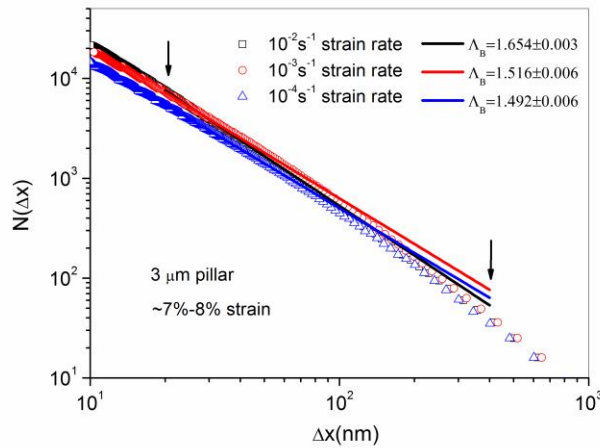
(c)

Figure 4 Box-counting analyses of the dislocation arrangements in the micropillars with different (a) size, (b) strain and (c) deformation strain rate.

In conclusion, dislocations are not retained in pillars smaller than 1 μm; on the contrary, in the larger samples, dislocation networks and even cells have been observed and a fractal geometry of dislocations evolves. The critical specimen size for the formation of a cell structure is similar to the size of the cells. Cell size decreases with increasing specimen size and strain. Cell formation appears not to depend very sensitively on strain rate. Strain bursts are caused by the collective escape of dislocations on one set of slip planes, resulting in the unravelling of the jammed dislocations stored during deformation. In agreement with previous reports, Schmid's Law is well obeyed in the 3 and 5 μm specimens, but rather more erratically

so in the 1 µm specimens. The Taylor work hardening mechanism fails in this regime and the strength of the micropillars is controlled by the mobility of the dislocations.

References

[1]   Z.W. Shan, R.K. Mishra, S.A.S. Asif, O.L. Warren, and A.M. Minor, Nat. Mater. 7 (2008) 115.

[2]   D. Kiener and A.M. Minor, Nano Lett. 11 (2011) 3816.

[3]   S.H. Oh, M. Legros, D. Kiener, and G. Dehm, Nat. Mater. 8 (2009), 95.

[4]   J.R. Greer, W.C. Oliver, and W.D. Nix, Acta Mater. 53 (2005) 1821.

[5]   M.D. Uchic and D.A. Dimiduk, Mater. Sci. Eng., A 400 (2005) 268.

[6]   K.S. Ng and A.H.W. Ngan, Acta Mater. 56 (2008) 1712.

[7]   D. Kiener and A.M. Minor, Acta Mater. 59 (2011) 1328.

[8]   A.H.W. Ngan, L. Zuo, and P.C. Wo, Proc. Roy. Soc. A462 (2006) 1661.

[9]   C.A. Volkert and E.T. Lilleodden, Philos. Mag. 86 (2006) 5567.

[10]   K.S. Ng and A.H.W. Ngan, Scripta Mater. 59 (2008) 796.

[11]   D.M. Dimiduk, M.D. Uchic, and T.A. Parthasarathy, Acta Mater. 53 (2005) 4065.

[12]   D. Kiener, M. Rester, S. Scheriau, B. Yang, R. Pippan, and G. Dehm, Int. J. Mater. Res. 98 (2007) 1047.

[13]   R. Gu, and A.H.W. Ngan, J. Mech. Phys. Solids 61 (2013) 1531.

[14]   A.S. Schneider, D. Kiener, C.M. Yakacki, H.J. Maier, P.A. Gruber, N. Tamura, M. Kunz, A.M. Minor, C.P. Frick, Mater. Sci. Eng. A 559 (2013) 147.

[15]   J.A. El-Awady, M.D. Uchic, P.A. Shade, S.-L. Kim, S.I. Rao, D.M. Dimiduk, C. Woodward, Scr. Mater. 68 (2013) 207.

[16]   T.A. Parthasarathy, S.I. Rao, D.M. Dimiduk, M.D. Uchic, and D.R. Trinkle, Scripta Mater. 56 (2007) 313.

[17]   Z.J. Wang, Q.J. Li, Z.W. Shan, J. Li, J. Sun, and E. Ma, Appl. Phys. Lett. 100 (2012) 071906.

[18]   F.F. Csikor, C. Motz, D. Weygand, M. Zaiser, and S. Zapperi, Science 318 (2007) 251.

[19]   X. Zhang and K.E. Aifantis, Mater. Sci. Eng., A 528 (2011) 5036.

[20]   M. Zaiser, K. Bay, and P. Hähner, Acta Mater. 47 (1999) 2463.

[21]   C.P. Frick, B.G. Clark, S. Orso, A.S. Schneider, and E. Arzt, Mater. Sci. Eng., A 489 (2008) 319.

[22]   D.M. Norfleet, D.M. Dimiduk, S.J. Polasik, M.D. Uchic, and M.J. Mills, Acta Mater. 56 (2008) 2988.

[23]   D. Kiener, W. Grosinger, G. Dehm, and R. Pippan, Acta Mater. 56 (2008) 580.

[24]   J.R. Greer and W.D. Nix, Phys. Rev. B 73 (2006) 245410.

[25]   D. Kiener, C. Motz, T. Schoberl, M. Jenko, and G. Dehm, Adv. Eng. Mater. 8 (2006) 1119.

[26]   C. Kirchlechner, D. Kiener, C. Motz, S. Labat, N. Vaxelaire, O. Perroud, J.-S. Micha, O. Uhlrich, O. Thomas, G. Dehm and J. Keckes, Phil. Mag. 91 (2011) 1256.

[27]   N. Hansen and D. Kuhlmann-Wilsdorf, Mater. Sci. Eng. 81 (1986) 141.

[28]   D.L. Holt, J. Appl. Phys. 41 (1970) 3197.